

Towards Secure and Practical Machine Learning via Secret Sharing and Random Permutation

Fei Zheng^a, Chaochao Chen^a, Xiaolin Zheng^{a,*} and Mingjie Zhu^b

^aCollege of Computer Science and Technology, Zhejiang University, Hangzhou, China,

^bJZTData Technology, Hangzhou, China,

ARTICLE INFO

Keywords:

Privacy-Preserving Machine Learning
Secret Sharing
Random Permutation
Multiparty Computation
Distance Correlation

ABSTRACT

With the increasing demand for privacy protection, privacy-preserving machine learning has been drawing much attention from both academia and industry. However, most existing methods have their limitations in practical applications. On the one hand, although most cryptographic methods are provable secure, they bring heavy computation and communication. On the other hand, the security of many relatively efficient privacy-preserving techniques (e.g., federated learning and split learning) is being questioned, since they are non-provable secure. Inspired by previous works on privacy-preserving machine learning, we build a privacy-preserving machine learning framework by combining random permutation and arithmetic secret sharing via our compute-after-permutation technique. Our method is more efficient than existing cryptographic methods, since it can reduce the cost of element-wise function computation. Moreover, by adopting distance correlation as a metric for evaluating privacy leakage, we demonstrate that our method is more secure than previous non-provable secure methods. Overall, our proposal achieves a good balance between security and efficiency. Experimental results show that our method not only is up to 5× faster and reduces up to 80% network traffic compared with state-of-the-art cryptographic methods, but also leaks less privacy during the training process compared with non-provable secure methods.

1. Introduction

Machine learning has been widely used in many real-life scenarios in recent years. In many practical cases, a good machine learning model requires data from multiple sources (parties). For example, two hospitals want to use their patients' data to train a better disease-diagnosis model, and two banks want to use their clients' data to train a more intelligent credit-ranking model. However, in many cases, the data sources are unwilling to share their data since their data is valuable or contains user privacy. Hence, how to train a model while keeping the privacy of sensitive data becomes a major challenge.

In traditional machine learning scenarios, data is *centralized* in a server or a cluster for model training. Two settings are usually encountered when privacy is taken into account [51]. One is that different data sources have different samples with the same set of features. In other words, data is *horizontally* distributed. Another setting is that data is *vertically* distributed, i.e., different data sources have overlapped samples but different features. Federated learning [31] mainly focuses on the horizontal setting. Privacy-Preserving Machine Learning (PPML) systems, e.g., [34, 48, 33], work for both settings via multiple data sources sharing data to one or several servers. In this paper, we aim to build a PPML system under the 3-server setting, which is suitable for both vertically and horizontally distributed data and supports both model training and inference.

In recent years, various methods have been proposed for privacy-preserving machine learning. These methods can be generally classified into two classes: *provable secure*

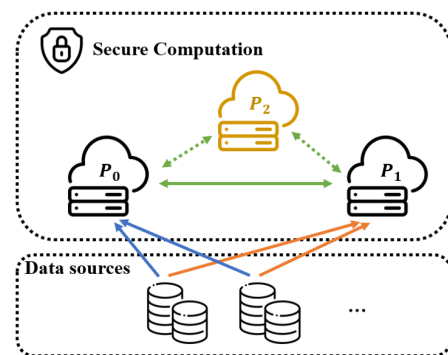


Figure 1: System overview.

methods and *non-provable secure* methods. Using provable secure methods, the adversary cannot derive any information about the input data within polynomial time under given threat models, e.g., *semi-honest* (passive) threat model and *malicious* (active) threat model [15]. In contrast, non-provable secure methods would leak certain information about the input data. Provable secure methods mainly use cryptographic primitives including Homomorphic Encryption (HE) [35, 17], Garbled Circuits (GC) [52], Secret Sharing (SS) [43], or other customized secure Multi-Party Computation (MPC) protocols [34, 10, 48, 33, 8, 16] to realize basic operations (e.g., addition, multiplication, comparison) of machine learning. Hence, their security can be formally proved. Non-provable secure methods include federated learning [31], split learning [47], and some hybrid methods [54, 50, 20, 55, 56]. Those methods are usually simple in theory and easy to implement. Another widely used technique is differential privacy [14], which protects

*Corresponding author.
ORCID(s):

privacy by adding certain noise in the specific stage of training or inference. However, it has a trade-off between privacy and accuracy and is mainly adopted in centralized or horizontal scenarios, and thus is out of the scope of this paper.

Although privacy-preserving machine learning has been widely studied, most existing methods have their limitations in practical applications. Cryptographic methods require heavy computation and communication and are always difficult to implement. Non-provable secure methods are usually very efficient, but they may leak privacy under certain conditions. Also, they lack quantification for privacy leakage. Existing researches indicate that some methods may leak information that can be exploited by the adversary [1, 49].

In this paper, we propose a practical method based on secret sharing and random permutation, which is more efficient than existing cryptographic methods and more secure than most non-provable secure methods. We present the system overview in Figure 1. From it, we can see that our method adopts a 3-server setting, i.e., the secure computation in our method involves three servers: P_0 , P_1 , and P_2 . First, all data sources upload their data to P_0 and P_1 in a secret-shared manner, which means that neither P_0 or P_1 has any meaningful information of the original data but random values. Then all three servers interactively perform model training or inference in an encrypted (secret-shared) manner. Finally, the desired output is reconstructed in plaintext.

Technically, our proposal adopts Arithmetic Secret Sharing (A-SS) scheme from previous work on MPC [10] and improves efficiency via the compute-after-permutation technique. For linear operations like addition and multiplication, our method behaves like [48, 38] where P_2 is used to generate beaver triples for secure multiplication. For non-linear element-wise functions like the widely used Sigmoid and ReLU, our method lets P_2 perform the computation via compute-after-permutation technique. Briefly speaking, P_2 gets a random permutation of the input from P_0 and P_1 , then computes the result of the element-wise function. After that, P_2 sends the shares of the computation result back to P_0 and P_1 .

The compute-after-permutation technique exploits the element-wise property of many activation functions. Unlike MPC methods, our method distributes the computation for element-wise functions to a server (P_2), hence greatly reduces computation and communication costs. To guarantee security, instead of sending plaintext to P_2 , a random permutation of the input is sent. We claim that the adversary can hardly extract any information of the original data from the compute-after-permutation technique, mainly due to two reasons. First, the number of permutations grows exponentially as the number of elements grows. Second, the input is already a random transformation of the original data (input of the model) since it has passed at least one neural network layer. Moreover, by quantitative analysis based on the statistical metric distance correlation [45] and simulated experiments, we show that our method leaks even less information than compressing the data into only one

dimension. Compared with non-provable secure methods like split learning [47] which directly reveal hidden representations, our method leaks far less privacy in terms of distance correlation.

The experiment results show that our method has less computation time and network traffic in logistic regression and neural network models compared with state-of-the-art cryptographic methods. Moreover, our method achieves the same accuracy as centralized training.

We summarize our main contributions in this paper as follows.

- We propose a secure and practical method for privacy-preserving machine learning, based on arithmetic sharing and the compute-after-permutation technique.
- We quantify privacy leakage and demonstrate the security of our method by using statistic measure distance correlation. We show that our method is more secure than existing non-provable secure methods.
- We benchmark our method with existing PPML systems on different models, and the results demonstrate that our method has less network communication and running time than centralized plaintext training, while achieving the same accuracy.

2. Related Work

We divide the methods for privacy-preserving machine learning into two groups. One is cryptographic methods that use cryptographic primitives to build PPML systems. Another is non-provable secure methods whose security cannot be proved in a cryptographic sense and may leak intermediate results during model training.

2.1. Cryptographic Methods

Cryptographic methods are based on cryptographic primitives such as GC, SS, HE, and MPC protocols. The security of these methods can be formally proved under their settings, i.e., no adversary can derive any information of the original data within polynomial time under the specific security setting.

The privacy problem is encountered with at least two parties. Hence, many PPML systems are built on a 2-server setting, where two servers jointly perform the computations of model inference or training. For example, CryptoNets [18] first used Fully Homomorphic Encryption (FHE) for neural network inference. ABY [10] provided a two-party computation protocol that supports computations including addition, subtraction, multiplication, and boolean circuit evaluation, by mixing arithmetic, boolean, and Yao sharing together. Motivated by ABY, SecureML [34] and MiniONN [28] mixed A-SS and GC together to implement privacy-preserving neural networks. Gazelle [23] avoided expensive FHE by using packed additive HE to improve efficiency and used GC to calculate non-linear activation functions.

The above two-party protocols are usually not efficient enough for practical applications, and many PPML systems used the 3-server or 4-server setting recently, where three or four parties jointly perform the PPML task. Under the 3-server setting, GC and HE are sometimes avoided due to their inefficiency. SecureNN [48] used a party to assist the most significant bit and multiplication on arithmetic shared values. ABY3 [33] performed three types of sharing in [10] under 3 parties to improve efficiency. Chameleon [38] used a semi-honest third-party for beaver triple generation and oblivious transfer. [6, 36, 4, 7, 25] developed new protocols based on arithmetic and boolean sharing under 3-server or 4-server settings and claim to outperform previous methods. Open-sourced PPML libraries, such as CryptFlow [26], TF-Encrypted [21], and Crypten [24] are also based on the semi-honest 3-servers setting where a certain party is usually used to generate Beaver triples.

Overall, cryptographic methods are aimed to design protocols that achieve provable security. They usually use SS as the basis, and develop new protocols for non-linear functions to improve efficiency.

2.2. Non-provable Secure Methods

We summarize the methods whose security cannot be formally proved in a cryptographic sense into non-provable secure methods. Those methods may use non-cryptographic algorithms and usually reveal certain intermediate results.

Federate learning and split learning are two well-known non-cryptographic methods. Federated learning [31] is commonly used in scenarios where data is horizontally distributed among multiple parties. It protects data privacy via sending model updates instead of original data to a server. Split learning [19, 47] is a straightforward solution for vertically distributed data. It simply splits the computation graph into several parts, while a server usually maintains the middle part of the graph as a coordinator. There are also other methods, for example: [20] designed a transformation layer that uses linear transformations with noises added on the raw data to protect privacy; [54] used additive HE for matrix multiplication but outsourced the activation function to different clients while keeping them unable to reconstruct the original input; [50] used a bayesian network to generate noisy intermediate results to protect privacy based on the *learning with errors* problem [37].

Non-provable methods usually leak certain intermediate results from joint computation. For example, federated learning leaks the model gradients, and split learning leaks the hidden representations. Their security depends on the security of certain intermediate results. However, those intermediate results can be unsafe. For example, [57, 53] show that the gradients can be used to reconstruct the original training samples, and [49] proved methods of [54, 50] can leak model parameters in certain cases. There have also been several attempts on the security of split learning. In this paper, since we focus on the computation of hidden layers, we compare our proposal with split learning in Section 5.

3. Preliminaries

In this section, we review the fundamental techniques of our method, including arithmetic secret sharing, random permutation, and distance correlation.

3.1. Arithmetic Secret Sharing

The idea of Secret Sharing (SS) [43] is to distribute a secret to multiple parties, and the secret can be reconstructed only when more than a certain number of parties are together. Hence, SS is widely used in MPC systems where 2 or 3 parties are involved. Arithmetic Secret Sharing (A-SS) is a kind of secret sharing that behaves in an arithmetic manner. When using A-SS, it is simple to perform arithmetic operations such as addition and multiplication on shared values. Due to its simplicity and information-theoretic security under semi-honest settings, it is widely used in different kinds of PPML systems [38, 48, 33].

We use the A-SS scheme proposed by [10] where a value is additively shared between two parties. The addition of two shared values can be done locally, while the multiplication of two shared values requires multiplicative triples introduced by Beaver [2]. To maintain perfect security, arithmetic sharing is performed on the integer ring \mathbb{Z}_{2^L} . The arithmetic operations we refer below are also defined on that ring by default.

Share: A value x is shared between two parties P_0, P_1 , which means that P_0 holds a value $\langle x \rangle_0$ while P_1 holds a value $\langle x \rangle_1$ such that $\langle x \rangle_0 + \langle x \rangle_1 = x$.

To share a value $x \in \mathbb{Z}_{2^L}$, party P_i (can be P_0, P_1, P_2 or any other party) simply picks $r \xrightarrow{\$} \mathbb{Z}_{2^L}$ and sends r and $x - r$ to P_0 and P_1 respectively.

Reconstruct: P_0 and P_1 both send their shares $\langle x \rangle_0, \langle x \rangle_1$ to some party P_i . The raw value $x = \langle x \rangle_0 + \langle x \rangle_1$ is reconstructed immediately on P_i by summing up the two shares.

Add: When adding a *public value* (values known to all parties) a to a shared value x , P_0 maintains $\langle x \rangle_0 + a$ and P_1 maintains $\langle x \rangle_1$. When adding a shared value a to a shared value x , two party add their shares respectively, *i.e.*, P_0 gets $\langle x \rangle_0 + \langle a \rangle_0$ and P_1 gets $\langle x \rangle_1 + \langle a \rangle_1$.

Mul/MatMul: When multiplying a shared value x with a public value a , the two parties multiply their shares of x with a respectively, *i.e.*, P_0 gets $\langle x \rangle_0 \cdot a$, P_1 gets $\langle x \rangle_1 \cdot a$. For multiplication of shared values, we use P_2 to generate beaver triples. When multiplying shared values x and y , P_2 generates beaver triples u, v, w , where u and v are randomly picked from \mathbb{Z}_{2^L} such that $w = u \cdot v$, and then shares them to P_0 and P_1 . Then P_0 and P_1 reconstruct $x - u$ and $y - v$ to each other. After that, P_0 calculates $(x - u)(y - v) + \langle (x - u)v \rangle_0 + \langle u(y - v) \rangle_0 + \langle w \rangle_0$, P_1 calculates $\langle (x - u)v \rangle_1 + \langle u(y - v) \rangle_1 + \langle w \rangle_1$. Then they get their shares of the result xy . Multiplication of matrices (MatMul) is performed similarly.

3.2. Random Permutation

Random permutation is used for privacy-preserving in many fields like data analysis [12], linear programming [11],

clustering [46], support vector machine [29, 30] and neural network [20]. It can be efficiently executed in a time complexity of $\mathcal{O}(n)$ [13].

The security of random permutation is based on that the number of possibilities grows exponentially with the number of elements. For example, for a vector of length 20, there are 2.43×10^{18} possible permutations, which means that the chances for the adversary to guess the original vector is negligible. We will present a more detailed analysis on the security of our proposed permutation method in Section 5.

3.3. Distance Correlation

Distance correlation [45] is used in statistics to measure the dependency between two random vectors. For two random vectors $X \in \mathbb{R}^p$ and $Y \in \mathbb{R}^q$, their distance correlation is defined as follows:

$$\text{Dcor}(X, Y) = \int_{\mathbb{R}^{p+q}} |f_{X,Y}(x, y) - f_X(x)f_Y(y)|^2 g(x, y) dx dy, \quad (1)$$

where f is the characteristic function and g is a certain non-negative weight function. The distance correlation becomes 0 when two random vectors are totally independent and 1 when one random vector is an orthogonal projection of the other one.

Let X and Y be n samples drawn from two distributions, their distance correlation can be estimated by

$$\text{Dcor}(X, Y) \approx \frac{V_n^2(X, Y)}{\sqrt{V_n^2(X, X)V_n^2(Y, Y)}}, \quad (2)$$

where $V_n^2(X, Y) = \frac{1}{n^2} \sum_{k,l=1}^n A_{kl}B_{kl}$ is the estimated distance covariance between X, Y (similar for $V_n^2(X, X)$ and $V_n^2(Y, Y)$). A_{kl} is the doubly-centered distances between A_k and A_l , and so is B_{kl} .

We use distance correlation as the measure of privacy leakage because it is concrete in the theory of statistics, easy to estimate, and intuitively reflects the similarity of topological structure between two datasets. Also, it is closely related to the famous Johnson-Lindenstrauss lemma [22], which states that random projections approximately preserve the distances between samples hence reserve the utility of the original data [3].

4. The Proposed Method

In this section, we first overview the high-level architecture of our method. Then we describe the building blocks of our method, i.e., fixed-point arithmetic and the compute-after-permutation technique. Finally, we combine the building blocks to realize the inference and training of neural networks.

4.1. Overview

Our method combines A-SS and random permutation to maintain the balance between privacy and efficiency. Similar

to existing work [48, 33], our method is based on the 3-server setting, where data is shared between two servers P_0 and P_1 , and is computed with the assist of P_2 , as has been illustrated in Section 1. Figure 2 displays the high-level architecture of our method.

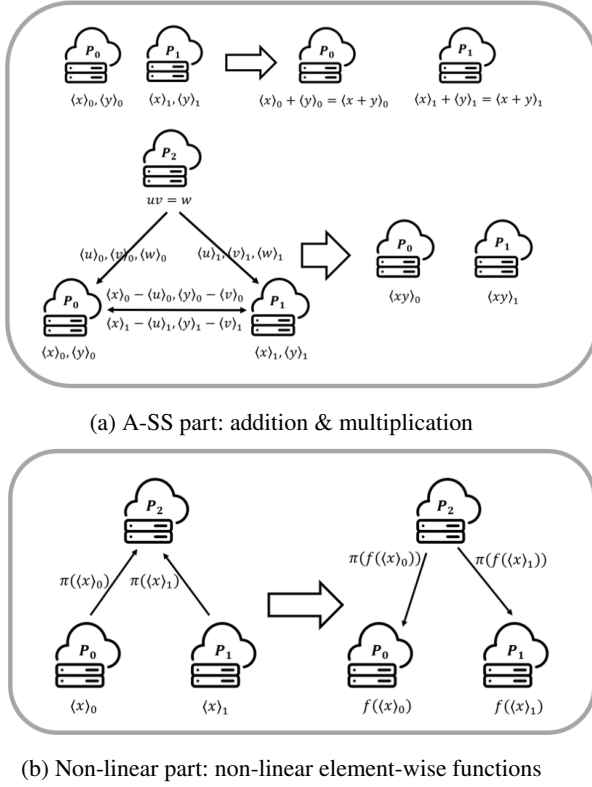
Since we use A-SS throughout the computation, all the values have to be converted to fixed-point. This is done via dividing the 64-bit integer into higher 41 bits and lower 23 bits. When converting a float-point value to fixed-point, the higher 41 bits are used for the integer part and the lower 23 bits are used for the decimal part. Linear operations like Add and Sub can be performed in an ordinary way, while the multiplication of shared values needs to be specially treated. We develop the ShareClip algorithm to avoid the error introduced by the shifting method in [34]. We will further discuss the details in Section 4.2.

In the semi-honest 3-server setting, addition and multiplication of the shared values can be easily implemented. In order to efficiently compute non-linear functions, we propose the *compute-after-permutation* technique. To compute the result of a non-linear element-wise function f on shared values \mathbf{x} , P_0 and P_1 first randomly permute their shares by a common permutation π to get $\pi[\mathbf{x}]$, then send them to P_2 . P_2 computes $f(\mathbf{x})$ and re-shares it to P_0 and P_1 . For element-wise functions, $f(\pi[\mathbf{x}]) = \pi[f(\mathbf{x})]$. Hence, P_0 and P_1 can use the inverse permutation to reconstruct the actual shared value of $f(\mathbf{x})$. We will further describe its details in Section 4.3.

In a fully connected neural network, each layer's computation contains a linear transformation and an activation function. The linear transformation (with bias) contains an addition (Add) and a matrix multiplication (MatMul), which can be done trivially under A-SS, as described above. As for activation functions, many of them including Sigmoid, ReLU, and Tanh are all element-wise, hence can be computed via the compute-after-permutation technique. There are also other operations like Transpose that are essential to the computation of neural networks. Those operations on shared values can be done locally on each party since they are not relevant to actual data values. Hence, after implementing those basic operations in a shared manner, we can build a shared neural network, which takes shared values as input and outputs shared results, piece by piece. We will describe the details for neural network inference and training in Section 4.4.

4.2. Fixed-Point Arithmetic

To maintain safety, A-SS is performed on the integer ring \mathbb{Z}_{2^L} . Since the computations in machine learning are in float-point format, we have to convert float-point numbers into fixed-point. A common solution is to multiply the float-point number by 2^p [34]. This conversion is naturally suitable for addition and subtraction of both normal values and shared values. However, for multiplication, the result needs to be truncated via shifting right by p bits. Considering multiplication of two numbers x and y , we have: $\lfloor xy \cdot 2^p \rfloor = (\lfloor x \cdot 2^p \rfloor \cdot \lfloor y \cdot 2^p \rfloor) / 2^p$ (with a small round-off error), where


Figure 2: Technique overview of our method.

$\lfloor \cdot \rfloor$ means to cast a real number into integer in ring \mathbb{Z}_{2^L} . For simplicity, the operators $+$, $-$ mentioned below are defined on the ring \mathbb{Z}_{2^L} . For negative values, we use $2^L - x$ to represent $-x$ where $x \in [1, 2^{L-1}]$.

For multiplication of shared values, the shifting method still can be adopted. As discussed in [34], the shifting method works for arithmetic shared values except for a very small probability of $\frac{1}{2^{L-1-2p}}$ for shifting error. Hence, some works [48, 32] directly adopted this method.

However, when a machine learning model (e.g., a neural network) becomes too complicated, the error rate will not be negligible anymore. For example, if we choose $p = 20$ and $L = 64$, the error rate is $\frac{1}{2^{13}}$. When performing linear regression inference with an input dimension of 100, there are 100 multiplications for each sample. Then the error rate of inference for one sample is about $\frac{1}{100}$. Obviously, such a high error rate is not acceptable.

Moreover, the shifting error could be very large and results in accuracy loss for machine learning models. Here we describe an example of shifting error. Let $L = 64$, $p = 20$, z is a result of multiplication before shifting, and $\langle z \rangle_0 = \langle z \rangle_1 = 2^{63} + 2^{20}$. Clearly, the desired result after shifting is $\frac{(2^{63} + 2^{20}) \times 2 \bmod 2^{64}}{2^{20}} = 2$ (since it is performed on integer ring $\mathbb{Z}_{2^{64}}$). In contrast, the simple shifting method introduced by [34] yields a result $\frac{2^{63} + 2^{20}}{2^{20}} \times 2 = 2^{43} + 1 +$

Algorithm 1: ShareClip

Input: Shared value X
Output: Clipped shared value Y

- 1 P_0 finds the indices of elements in $\langle X \rangle_0$ that are greater than 2^{L-2} as *indices_overflow* and the indices of elements that are smaller than -2^{L-2} as *indices_underflow*, and then sends them to P_1 ;
 - 2 P_0 and P_1 copy X to Y ;
 - 3 **for** *index* in *indices_overflow* **do**
 - 4 P_0 set $\langle Y \rangle_0[\textit{index}] \leftarrow \langle Y \rangle_0[\textit{index}] - 2^{L-2}$;
 - 5 P_1 set $\langle Y \rangle_1[\textit{index}] \leftarrow \langle Y \rangle_1[\textit{index}] + 2^{L-2}$;
 - 6 **end**
 - 7 **for** *index* in *indices_underflow* **do**
 - 8 P_0 set $\langle Y \rangle_0[\textit{index}] \leftarrow \langle Y \rangle_0[\textit{index}] + 2^{L-2}$;
 - 9 P_1 set $\langle Y \rangle_1[\textit{index}] \leftarrow \langle Y \rangle_1[\textit{index}] - 2^{L-2}$;
 - 10 **end**
-

$2^{43} + 1 = 2^{44} + 2$. We can see that since this error is caused by overflow/underflow, and thus is very large. In experiments, we also noticed that this error caused the model training to be very unstable, unable to achieve the same performance as centralized plaintext training.

Some work [10, 33, 38] proposed to share conversion protocols to overcome this problem. However, since our method does not involve any other sharing types except A-SS, the share conversion is not suitable.

Our solution to this problem is to let each party clip its share so that the signs of their shared values are opposite. By doing this, we can avoid the error in the shifting method. We term it as ShareClip. We prove that when the real value x is within a certain range, this clipping method can prevent all underflow/overflow situations encountered in truncation.

Theorem 1. *If a shared value x on ring \mathbb{Z}_{2^L} satisfies $x \in [-2^{L-2}, 2^{L-2})$, and $\langle x \rangle_0 \in [-2^{L-2}, 2^{L-2})$,*

$$\textit{then } \lfloor \frac{\langle x \rangle_0}{2^p} + \frac{\langle x \rangle_1}{2^p} \rfloor \in [\lfloor \frac{x}{2^p} \rfloor - 1, \lfloor \frac{x}{2^p} \rfloor + 1].$$

PROOF. Obviously $\langle x \rangle_1 \in [-2^{L-1}, 2^{L-1})$ and no overflow/underflow is encountered when computing $\langle x \rangle_0 + \langle x \rangle_1$. Suppose $\frac{x}{2^p} = c$, $\frac{\langle x \rangle_0}{2^p} = a$, $\frac{\langle x \rangle_1}{2^p} = b$, we can easily obtain the result from the fact that if $a + b = c$, $\lfloor a \rfloor + \lfloor b \rfloor \in [\lfloor c \rfloor - 1, \lfloor c \rfloor + 1]$.

We describe our proposed ShareClip protocol in Algorithm 1. Its basic idea is that two party interactively shrink their shares when the absolute values of shares are too large. Notably, it can be executed during Mul/MatMul of shared values without any extra communication rounds.

Choice of L and p . For ease of implementation, we set $L = 64$, since 64-bit integer operations are widely supported by various libraries. In order to preserve precision for fixed-point computation, we set the precision bits $p = 23$ as suggested in [9]. Besides, to avoid overflow/underflow during multiplication while using our ShareClip algorithm, all input

and intermediate values during computation must be within the range $[-2^{40}, 2^{40})$.

4.3. Compute-After-Permutation

Activation functions are essential for general machine learning models such as logistic regression and neural networks. In a fully connected neural network, they always come after a linear layer. Due to their non-linearity, they cannot be directly computed via A-SS. To solve this problem, some methods use GC [34, 28], while others use customized MPC protocols [33, 48]. However, those methods are usually expensive in implementation, computation and communication. Moreover, they usually use approximations to compute non-linear functions, which may cause accuracy loss.

In contrast, our proposed *compute-after-permutation* method is quite efficient and easy to implement. Since most activation functions are element-wise, we simply randomly permute the input values and let P_2 compute the results. Randomly permuting n elements yields $n!$ possible outcomes. Hence, even a few elements can have a huge number of permutations. During the training and inference of machine learning models, input data is always fed in batches, where multiple samples are packed together. Besides, the dimension of each input could be large. Therefore, the inputs of activation functions are always of large size. As a consequence, when P_2 gets those permuted hidden representations, it has little chance to guess the original hidden representation, and also little knowledge about the original data. We will further analyze its security in Section 5.

We formalize the compute-after-permutation technique in Algorithm 2, and describe it as follows: take neural network for example, assume that P_0 and P_1 already calculated the shared hidden output \mathbf{z} . First, P_0 and P_1 use their common Pseudorandom Generator (PRG) to generate a random permutation π (line 10). Then they permute their shares and get $\pi[\langle \mathbf{z} \rangle_0]$ and $\pi[\langle \mathbf{z} \rangle_1]$ (line 11). After this, they both send the permuted shares to P_2 . When P_2 receives these shares, it reconstructs $\pi[\mathbf{z}]$ by adding them up (line 12). Then P_2 decodes $\pi[\mathbf{z}]$ to its corresponding float value and uses ordinary ways to compute the activation $f(\pi[\mathbf{z}])$ easily (line 13~14). After encoding $f(\pi[\mathbf{z}])$ into fixed point, P_2 needs to reshape it to P_0 and P_1 . To do it, P_2 picks a random value $\mathbf{r} \leftarrow \mathbb{Z}_{2^L}^{\text{Shape}(\mathbf{z})}$ with the same shape of \mathbf{z} (line 15), then sends \mathbf{r} to P_0 and $\pi[\mathbf{z}] - \mathbf{r}$ to P_1 (line 16). Then P_0 and P_1 use the inverse permutation π^{-1} to get $\pi^{-1}[\mathbf{r}]$ and $f(\mathbf{z}) - \pi^{-1}[\mathbf{r}]$ respectively (line 17). Thus, they both get their shares of $f(\mathbf{z})$.

Enhancing Security via Random Flipping. Hidden representations are already the transformations of the original data since at least one prior layer is passed. Hence, the permutation of hidden representation does not leak the value sets of the original data. However, many neural networks still have an activation on the final prediction layer. In many tasks, the dimension of the label is just one. For example, when a bank wants to predict the clients' possibility of credit default, the label is 0 or 1 (not default or default), and when

a company wants to predict the sales of products, the label is also one-dimensional and probably between 0 and 1 because normalization is used in the preprocessing. In those cases, random permutation only shuffles the predictions within a batch, but the set of the predictions is still preserved. Hence, P_2 can learn the distribution of the predictions in each batch. Considering that the predictions can be close to the label values in training or inference, the distribution of the predictions is also sensitive and needs to be protected.

In order to prevent this potential information leakage, we propose to add random flipping to the random permutation. Assume $\mathbf{z} \in \mathbb{R}^B$ is the output of the last layer. Before applying the random permutation π to it, we first generate a random mask $\mathbf{m} \stackrel{\$}{\leftarrow} \{0, 1\}^B$. Then, for each element in \mathbf{z} , if the corresponding mask is 1, we change it to its negative. Notice that for Sigmoid, we have $\text{Sigmoid}(-x) = 1 - \text{Sigmoid}(x)$, and for Tanh, we have $\text{Tanh}(-x) = -\text{Tanh}(x)$. Hence, P_0 and P_1 can easily get the real value of $f(\mathbf{z})$ from P_2 's result. The random flipping mechanism is summarized in lines 2~9 and 18~25 of Algorithm 2.

Improving Communication via Common Random Generator. To reduce the communication for multiplications, [38] used a PRG shared between P_1 and P_2 . We also adopt this method for multiplication and further extend this method to our compute-after-permutation technique. At the offline stage, P_1 and P_2 set up a common PRG *prg*. As mentioned above, after P_2 computed the results of element-wise functions, it generates a random vector \mathbf{r} as P_1 's share. In order to reduce communication, \mathbf{r} is generated by *prg*. Because P_1 has the same PRG, P_2 does not need to send \mathbf{r} to P_1 . This helps to reduce the network traffic of element-wise functions from $4NL$ bits to $3NL$ bits, where N is the number of elements in the input. We compare our compute-after-permutation technique with the state-of-the-art MPC protocols on ReLU function in Table 1. Theoretical result shows that compute-after-permutation requires fewer communication rounds and less network traffic than existing MPC protocols.

4.4. Neural Network Inference and Training

Based on A-SS and the compute-after-permutation techniques, we can implement both inference and training algorithms for general machine learning models such as fully connected neural networks. The operations required for neural network inference and training can be divided into three types:

- Linear operations: Add, Sub, Mul, and MatMul;
- Non-linear element-wise functions: Relu, Sigmoid, and Tanh;
- Local transformations: Transpose.

We have already implemented linear operations and non-linear element-wise functions by A-SS and the compute-after-permutation technique. As for the Transpose operator, it can be trivially achieved by P_0 and P_1 through transposing

Algorithm 2: Compute-after-Permutation(CAP)

Input: Shared value Z ,
Element-wise function
 $f \in \{\text{Relu}, \text{Sigmoid}, \text{Tanh}\}$,
Flipping $\in \{\text{True}, \text{False}\}$

Output: Shared element-wise function result
 $Y = f(Z)$

- 1 P_0 and P_1 flatten Z to a one-dimensional vector \mathbf{z} ;
- 2 **if** Flipping = True **then**
- 3 **if** $f \notin \{\text{Sigmoid}, \text{Tanh}\}$ **then**
- 4 **return** Error;
- 5 P_0 and P_1 generate a random mask with the
same size of \mathbf{z} : $\mathbf{m} \xleftarrow{\$} \{0, 1\}^{\text{Size}(\mathbf{z})}$;
- 6 **for** $i = 1$ to $\text{Size}(\mathbf{z})$ **do**
- 7 **if** $m_i = 1$ **then**
- 8 P_0 and P_1 compute $z_i \leftarrow -z_i$ by negate
their shares;
- 9 **end**
- 10 P_0 and P_1 generate a random permutation
 $\pi = j_1 j_2 \dots j_n$ using their common PRG;
- 11 P_0 and P_1 permute their shares of \mathbf{z} respectively,
generate new shared value $\mathbf{z}' = (z_{j_1}, z_{j_2}, \dots, z_{j_n})$;
- 12 P_0 and P_1 reconstruct \mathbf{z}' to P_2 ;
- 13 P_2 gets \mathbf{z}' then decodes it to its float-point value \mathbf{z}'_f ;
- 14 P_2 computes element-wise function result
 $\mathbf{y}'_f = f(\mathbf{z}'_f)$ and encodes it to fixed-point value \mathbf{y}' ;
- 15 P_2 generates a random vector $\mathbf{r} \xleftarrow{\$} \mathbb{Z}_{2^L}^{\text{Size}(\mathbf{z})}$
- 16 P_2 sends \mathbf{r} to P_0 and $\mathbf{y}' - \mathbf{r}$ to P_1 ;
- 17 P_0 and P_1 apply the inverse permutation π^{-1} to
their shares of \mathbf{y}' and get new shared value \mathbf{y} ;
- 18 **if** Flipping = True **then**
- 19 **for** $i = 1$ to $\text{Size}(\mathbf{z})$ **do**
- 20 **if** $m_i = 1$ **then**
- 21 **if** $f = \text{Sigmoid}$ **then**
- 22 P_0 and P_1 compute $y_i \leftarrow \text{Sub}(1, y_i)$;
- 23 **if** $f = \text{Tanh}$ **then**
- 24 P_0 and P_1 compute $y_i \leftarrow -y_i$;
- 25 **end**
- 26 P_0 and P_1 reshape \mathbf{y} to the shape of Z to get Y ;

their shares locally without any communication. All these operators have inputs and outputs as secret shared values. Hence, using those operators, we can implement neural network inference and training algorithms, as described in Algorithm 3 and Algorithm 4. Notably, the Sum is performed similarly as Add, and the differentiation of activation function ($\frac{da}{dx}$) can be the combination of the implemented operators (functions).

5. Security Analysis

We adopt the semi-honest (honest-but-curious) setting in this paper, where each party will follow the protocol but

Table 1

Comparison of communication rounds and traffics with existing MPC protocols on ReLU function, where p is some prime number and k is the security parameter for GC which is usually more than 128.

Protocol	Rounds	Bits
Ours	3	$3L$
SecureNN[48]	11	$8L \log p + 32L + 2$
ABY3[33]	$6 + \log L$	$105L$
Trident[7]	7	$16L + 64$
GC[39]	4	$k(3L - 1)$

Algorithm 3: NN-Infer

Input: Shared batch data X ,
Shared network parameters (weights, bias,
activations) $\{W_i, \mathbf{b}_i, a_i\}$

Output: Network output Y

- 1 $A_0 = X$;
- 2 **for** i from 0 to $\text{num_layers} - 1$ **do**
- 3 $Z_{i+1} \leftarrow \text{Add}(\text{MatMul}(A_i, W_i), \mathbf{b}_i)$;
- 4 $A_{i+1} \leftarrow \text{CAP}(Z_{i+1}, a_i, (i = \text{num_layers} - 1))$;
- 5 **end**
- 6 $Y \leftarrow A_{\text{num_layers}}$

Algorithm 4: NN-Backprop

Input: Shared batch data X ,
Shared label Y ,
Shared network parameters $\{W_i, \mathbf{b}_i, a_i\}$,
Learning rate lr

Output: Network output Y

- 1 $\hat{Y} \leftarrow \text{NN-Infer}(X, \{W_i, \mathbf{b}_i, a_i\})$;
- 2 $g_{\text{num_layers}} \leftarrow \text{Mul}(2, \text{Sub}(Y, \hat{Y}))$;
- 3 **for** i from $\text{num_layers} - 1$ to 0 **do**
- 4 $g_{i+1} \leftarrow \frac{da_{i+1}}{dx}(A_{i+1}) \cdot g_{i+1}$;
- 5 $g_i \leftarrow \text{MatMul}(g_{i+1}, \text{Transpose}(W_i))$;
- 6 $\mathbf{b}_i \leftarrow \mathbf{b}_i - lr \cdot \text{Sum}(g_i, \text{axis} = 0)$;
- 7 $W_i \leftarrow W_i - lr \cdot \text{MatMul}(\text{Transpose}(A_i), g_i)$;
- 8 **end**

try to learn as much information as possible from his own view [15]. In reality, P_0 and P_1 are data holders while P_2 can be a party that both P_0 and P_1 trust, e.g., a privacy-preserving service provider, a server controlled by government. And since in our method, the computation of P_2 is simple, it is convenient to put P_2 into a TEE (Trusted Execution Environment) [41] device to enhance security.

The security of linear and multiplication operations of A-SS values is proved to be secure under this setting in previous work [48] using the universal composability framework [5]. Here, we only need to demonstrate the security of the compute-after-permutation technique.

To do this, we will first empirically study the insecurity of directly revealing hidden representations and explain why

compute-after-permutation is practically secure. Then we will quantitatively analyze the distance correlation between the data obtained by P_2 and the original data with or without random permutation. We will also derive a formula of expected distance correlation for certain random linear transformations, and an estimation for random permutations.

5.1. Insecurity of Directly Revealing Hidden Representations

Since our method is mainly based on the permutation of hidden representations, here we demonstrate the insecurity of the methods that directly reveal the hidden representations such as split learning [47]. The security guarantee of split learning is the non-reversibility of hidden representations. For a fully connected layer, the hidden representation (i.e. the output of that layer) can be considered as a random projection of the input. For example, the first layer's output is $Y = XW$ (without bias), where $X \in \mathbb{R}^{B \times D}$ is the original data and $W \in \mathbb{R}^{D \times H}$ is the transformation matrix. Anyone who gets Y cannot guess the exact value of X and W due to there are infinite choices of X' and W' that can yield the same product $X'W' = XW$. Thus, it is adopted by existing works like [54, 47, 20].

However, although the adversary cannot directly reconstruct the original data from hidden representations, there are still potential risks of privacy leakage. For example, [49] has proven that the methods in [50, 54] may leak information about the model weights when the adversary uses specific inputs and collects the corresponding hidden representations. [1] used distance correlation to show that when applying split learning to CNN, the hidden representations are highly correlated with the input data. Moreover, the input data may be reconstructed from hidden representations. Older researches like [42] also suggested that it is possible to reconstruct original data from its random projection with some auxiliary information. Besides, the non-reversibility of random projection only protects the original data, but not the utility of data [3]. Suppose that company A and company B jointly train a model via split learning, where the training samples are provided by A and the label is provided by B. B can secretly collect the hidden representations of the training samples during training. Then B can either use those hidden representations on another task or give them to someone else without A's permission.

In order to show the insecurity of revealing hidden representation and the effectiveness of random permutation, we propose a simple attack based on the histogram of distances. The purpose of the attack is to find similar samples according to a certain hidden representation. Since Johnson-Lindenstrauss lemma [22] states that random projection can approximately preserve distances between samples, it is natural that the histogram before and after random projection can be similar. Hence, for one sample \mathbf{y} in a projected set $Y = XW$, the adversary first computes the distances between \mathbf{y} and any other sample \mathbf{y}' , and then draws the histogram of those distances. If the adversary has a dataset X' with the same distribution of the original dataset X , it then

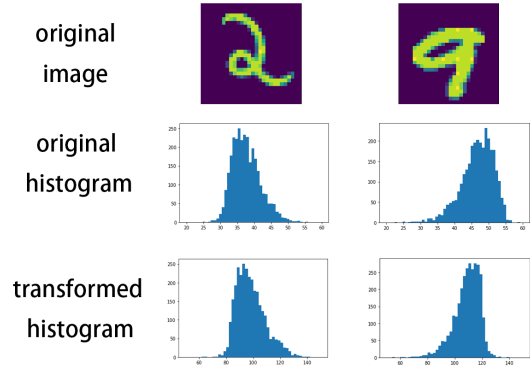


Figure 3: The histogram of distances are similar after linear transformation.

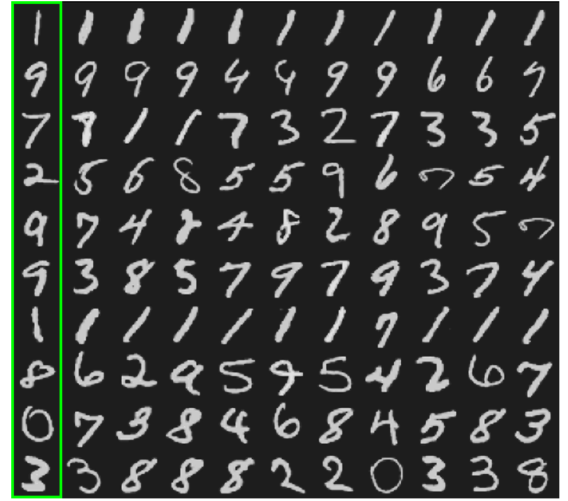


Figure 4: By comparing histograms of distances, we can find the similar samples from X' (the most left column is the original sample in X , and the other columns are the top-10 similar samples found in X').

can find the samples in X' which have similar histograms with \mathbf{y} . Those samples are similar with the original sample corresponding to \mathbf{y} . We name this simple attack as *histogram attack*.

We now use the MNIST [27] dataset as an example. Assume the adversary has 3,000 images randomly chosen from the MNIST dataset, along with 128-dimensional hidden representations of 3,000 other images from the dataset. As shown in Figure 3, the histograms of distances before and after random projection are somewhat similar. The adversary randomly chooses 10 projected vectors and finds their top-10 most similar samples based on the histogram using earth mover's distance [40]. We present the original image and the similar images found via histograms in Figure 4. Obviously, those top-10 images are quite similar to the original one. For example, for the images of digit 1, almost all of the top-10 similar images are actually of digit 1.

We conclude that directly revealing the hidden representations has two major security concerns:

- It preserves the utility of the original data, and may be used multiple times without the permission of data sources.
- It preserves the topological structure of the dataset to some extent. If the adversary knows the distribution of the original data, it can find similar samples corresponding to the hidden representation.

5.2. Security of Compute-after-Permutation

The compute-after-permutation technique is mainly based on random permutation, while for model predictions, random flipping is used. We demonstrate that random permutation can protect the original data, and the random flipping can protect the model predictions and the label.

Random Permutation Protects the Original Data. Random permutation is a simple technique with strong privacy-preserving power. Even with a set of very few elements, there are an extremely large number of possible permutations. E.g., 10 distinct elements have more than 3 million permutations, while with 20 distinct elements the number of permutations scales to the magnitude of 10^{18} . Hence, under a mild assumption that the hidden representation of the original data batch has at least a few distinct elements, it is impossible for the adversary to guess the original hidden representation from its random permutation.

A disadvantage of random permutation is that it preserves the set of elements. However, our method is not affected by this disadvantage mainly for two reasons:

- In our method, the permutation is performed on the hidden representations instead of the original data, the set of original data values are not exposed.
- During the training and inference of machine learning models, the data is always fed in batches. The random permutation is performed on the whole batch of hidden representations. Hence, the elements in different samples' hidden representations are mixed together, making it hard to extract any individual sample's information.

In order to measure the privacy-preserving power of random permutation more precisely, we will quantify the privacy leakage of random permutation and linear transformation measured by distance correlation in the following section 5.3. By quantitative computation and simulated experiments, we demonstrate that applying random permutation on hidden representations usually leaks less privacy than reducing the hidden representations' dimension into 1.

Random Flipping Protects Predictions and Label. The security of random flipping is based on that no matter what the original prediction is, the adversary will get a value with an equal probability of being positive or negative. We denote the original predictions by \mathbf{z} and the flipped predictions by

\mathbf{z}' , and we have:

$$\begin{aligned} P(z'_i < 0) &= P(z'_i < 0 | z_i < 0)P(z_i < 0) + P(z'_i < 0 | z_i \geq 0)P(z_i \geq 0) \\ &= \frac{1}{2}P(z_i < 0) + \frac{1}{2}P(z_i \geq 0) = \frac{1}{2} = P(z'_i \geq 0). \end{aligned} \quad (3)$$

Hence, no matter what the original predictions are, P_2 only receives a batch of values with equal probabilities of negative or positive. When the label is binary, no information about the label is leaked. When the label is continuous, the scales of the predictions are leaked. However, since the predictions do not exactly match the label and the values are permuted, we consider those flipped values are safe to reveal.

As discussed above, with the random permutation performed on hidden representation, the adversary cannot reconstruct the original hidden representation and very little information about the original data is leaked. Also, the random flipping preserves the privacy for model predictions and the label data. Therefore, we conclude that our compute-after-permutation technique is practically secure.

5.3. Quantitative Analysis on Distance Correlation

To better illustrate the security of our compute-after-permutation method, we quantify the privacy leakage by distance correlation. First, we derive a formula of expected distance correlation for random linear transformation. Then we demonstrate that random permuted vector can be viewed as the combination of element-wise mean of the vector and an almost-random noise. Based on this, we conclude that random permutation usually preserves more privacy than compressing data samples to only one dimension. We also conduct experiments on 4 simulated data distributions to verify our conclusion.

In the following of this section, we use $\|\mathbf{x}\|$ to denote the euclidean norm of the vector \mathbf{x} , upper case letters such as X to denote the corresponding random variable, and x_i to denote the i 'th component of the vector.

5.3.1. Linear Transformation

Theorem 2 (DCOR for linear transformations). *Suppose $X \in \mathbb{R}^n$ is an arbitrary random vector, and let $Y = AX$, where $A \in \mathbb{R}^{n \times d}$ is the transformation matrix that satisfies the probability of $P(A) = P(AT)$ for any orthogonal matrix T (i.e., P is a rotation-invariant distribution), then*

$$\mathbb{E}_A[Dcor(X, Y)] = \sqrt{\frac{a^2(S_1 + S_2 - 2S_3)}{a^2S_1 + b^2S_2 - 2S_3'}}, \text{ where}$$

$S_1 = \mathbb{E}\|X - X'\|^2$, $S_2 = \mathbb{E}\|X - X'\|^2$, $S_3 = \mathbb{E}\|X - X'\|X - X''\|$, $S_3' = \mathbb{E}\|X - X'\|AX - AX''\| = \mathbb{E}C(X - X', X - X'')$, X', X'' are identical independent distributions of X ,

and

$$a = \mathbb{E}_A \frac{|\mathbf{A}\mathbf{u}|}{|\mathbf{u}|}, b = \sqrt{\mathbb{E}_A \frac{|\mathbf{A}\mathbf{u}|^2}{|\mathbf{u}|^2}},$$

$$C(\mathbf{x}, \mathbf{y}) = \mathbb{E}_A [g_A(\theta(\mathbf{x}, \mathbf{y}))|\mathbf{x}||\mathbf{y}|],$$

$g_A(\theta) = \mathbb{E}_A \left[\frac{|\mathbf{A}\mathbf{x}||\mathbf{A}\mathbf{y}|}{|\mathbf{x}||\mathbf{y}|} \right]$ where \mathbf{x}, \mathbf{y} denote arbitrary vectors and θ denotes the angle between them.

PROOF. The proof yields directly from the Brownian distance covariance [44] formula and the rotation-invariant property of A .

Corollary 1. The function $g_A(\theta)$ is monotonic decreasing for $\theta \in [0, \pi/2]$.

PROOF. Due to the rotation-invariant property of A , it is sufficient to assume $\mathbf{x} = \begin{bmatrix} \cos \theta/2 \\ \sin \theta/2 \\ \mathbf{0} \end{bmatrix}, \mathbf{y} = \begin{bmatrix} \cos \theta/2 \\ \sin -\theta/2 \\ \mathbf{0} \end{bmatrix}$, then we have $g_A(\theta) = \mathbb{E}_A |\mathbf{A}\mathbf{x}||\mathbf{A}\mathbf{y}|$.

By rotating A in the plane spanned by the first two axis, we have $AT = A \begin{bmatrix} \cos \alpha & \sin \alpha & O \\ -\sin \alpha & \cos \alpha & O \\ O & O & E \end{bmatrix}$. Then we have:

$$\begin{aligned} \mathbb{E}_A [|\mathbf{A}\mathbf{x}||\mathbf{A}\mathbf{y}|] &= \mathbb{E}_A [|\mathbf{A}T\mathbf{x}||\mathbf{A}T\mathbf{y}|] = \mathbb{E}_A \mathbb{E}_T [|\mathbf{A}T\mathbf{x}||\mathbf{A}T\mathbf{y}|] \\ &= \mathbb{E}_A \mathbb{E}_\alpha \left[|\cos(\alpha - \theta/2)\mathbf{a}_0 - \sin(\alpha - \theta/2)\mathbf{a}_1| \right. \\ &\quad \left. \cdot |\cos(\alpha + \theta/2)\mathbf{a}_0 - \sin(\alpha + \theta/2)\mathbf{a}_1| \right] \end{aligned} \quad (4)$$

, where \mathbf{a}_0 and \mathbf{a}_1 are first two columns of A .

By taking its derivation on θ , we have:

$$\begin{aligned} \frac{d \mathbb{E}_T |\mathbf{A}T\mathbf{x}||\mathbf{A}T\mathbf{y}|}{d\theta} &= -(|\mathbf{a}_0|^2 + |\mathbf{a}_1|^2) \sin \theta \cdot \\ &\int_{\alpha=0}^{2\pi} \text{sign} [\cos 2\alpha(|\mathbf{a}_0|^2 - |\mathbf{a}_1|^2) - \sin 2\alpha(\mathbf{a}_0 \cdot \mathbf{a}_1) \\ &\quad + (|\mathbf{a}_0|^2 + |\mathbf{a}_1|^2) \cos \theta] d\alpha. \end{aligned} \quad (5)$$

The first two terms inside the sign function always integral to zero, and the third term is a constant positive term. Hence Eq. (5) is non-positive when $\theta \in [0, \pi/2)$, regardless of A .

The above analysis shows that the expected distance correlation between the original data and random linear transformed data is affected by the distribution of the original data. Since the coefficients a, b in Theorem 2 are constant, the expected distance correlation mainly relies on term S'_3 , which is a function of angles between different data points. Larger angle leads to smaller distance correlation.

Intuitively, larger angle means data points are distributed more randomly on each dimension, and smaller angle indicates data points are concentrated on some subspaces. For example, if all data points are distributed very near to a line,

then all angles between $\mathbf{x} - \mathbf{x}'$ and $\mathbf{x} - \mathbf{x}''$ ($\mathbf{x}, \mathbf{x}', \mathbf{x}''$ are three data points) are near to 0, which leads to a large distance correlation.

For neural networks, the transformation matrix $A \in \mathbb{R}^{d \times h}$ is initialized with normal distribution $\mathcal{N}(0, \sigma^2)$, which satisfies the rotation-invariant property. In this case, we have $a = \sigma \sqrt{2} \frac{\Gamma((h+1)/2)}{\Gamma(h/2)}$, $b = \sigma \sqrt{h}$, and $g_A(\theta) =$

$$\int_{\mathbf{x}, \mathbf{y} \in \mathbb{R}^d} e^{-\frac{|\mathbf{x}|^2 + |\mathbf{y}|^2}{2\sigma^2}} |\mathbf{x}| |\cos \theta \mathbf{x} + \sin \theta \mathbf{y}| d\mathbf{x} d\mathbf{y}.$$

5.3.2. Random Permutation

For a vector $\mathbf{x} \in \mathbb{R}^n$, we write its random permutation as $\pi[\mathbf{x}]$ which has the following properties:

- $\mathbb{E}_\pi \pi[\mathbf{x}] = [\mathbb{E} \mathbf{x}, \dots, \mathbb{E} \mathbf{x}] = M(\mathbf{x})$, where $\mathbb{E} \mathbf{x} = \frac{1}{n} \sum_{i=1}^n \mathbf{x}_i$.
- $(\pi[\mathbf{x}] - \mathbb{E}_\pi \pi[\mathbf{x}])^T \mathbf{1} = 0$ for any π .
- $\left| \pi[\mathbf{x}] - \mathbb{E}_\pi \pi[\mathbf{x}] \right| = \left| \mathbf{x} - \mathbb{E}_\pi \pi[\mathbf{x}] \right|$ for any π .

In other words, the permuted vector can be viewed as a sum of the element-wise mean vector $M(\mathbf{x})$ and an error vector $\mathbf{e}_x = \pi[\mathbf{x}] - \mathbb{E}_\pi \pi[\mathbf{x}]$. The error vector is distributed on a $(n-1)$ -sphere on a hyperplane orthogonal to $\mathbf{1}$ centered at origin $\mathbf{0}$. We further illustrate that this error vector is approximately uniformly distributed on that sphere.

Theorem 3. The error vector's projection on any unit vector on the hyperplane $\mathbf{y}^T \mathbf{1} = 0$ has a mean 0 and a variance of $\approx \frac{1}{n} |\mathbf{e}_x|^2$.

PROOF. The mean of $\mathbf{e}_x \cdot \mathbf{y}$ can be computed as follows:

$$\mathbb{E} [\mathbf{e}_x \cdot \mathbf{y}] = \mathbb{E} \sum_{i=1}^n \pi_x [\mathbf{e}_x]_i \mathbf{y}_i = \sum_{i=1}^n \mathbb{E}_{\pi_x} \pi_x [\mathbf{e}_x]_i \cdot \mathbf{y}_i = \mathbb{E}_{\pi_x} \mathbf{0} \cdot \mathbf{y}_i = 0.$$

For the calculation of variance, we have:

$$\text{Var} [\mathbf{e}_x \cdot \mathbf{y}] = \mathbb{E}_{\pi_x} \sum_{i,j=1}^n \pi_x [\mathbf{e}_x]_i \mathbf{y}_i \pi_x [\mathbf{e}_x]_j \mathbf{y}_j. \quad (6)$$

The term inside sum can be divided into two cases:

- $i = j$: In this case, $\mathbb{E}_{\pi_x} \pi_x [\mathbf{e}_x]_i \mathbf{y}_i \pi_x [\mathbf{e}_x]_j \mathbf{y}_j = \mathbb{E}_{\pi_x} \pi_x [\mathbf{e}_x]_i^2 \mathbf{y}_i^2 = \frac{|\mathbf{e}_x|^2}{n} \mathbf{y}_i^2$.
- $i \neq j$: In this case, $\mathbb{E}_{\pi_x} \pi_x [\mathbf{e}_x]_i \mathbf{y}_i \pi_x [\mathbf{e}_x]_j \mathbf{y}_j = \mathbb{E}_{\pi_x} \pi_x [\mathbf{e}_x]_i \pi_x [\mathbf{e}_x]_j \mathbf{y}_i \mathbf{y}_j$. Observed that $\mathbb{E}_{\pi_x} \pi_x [\mathbf{e}_x]_i \pi_x [\mathbf{e}_x]_j = \frac{1}{n^2} \sum_{i \neq j} (\mathbf{e}_x)_i (\mathbf{e}_x)_j = \frac{1}{n^2} \sum_i -(\mathbf{e}_x)_i^2 = -\frac{1}{n^2} |\mathbf{e}_x|^2$, we have: $\mathbb{E}_{\pi_x} \pi_x [\mathbf{e}_x]_i \mathbf{y}_i \pi_x [\mathbf{e}_x]_j \mathbf{y}_j = -\frac{1}{n^2} |\mathbf{e}_x|^2 \mathbf{y}_i \mathbf{y}_j$.

Then by replacing those terms in Eq. (6) and notice that $\sum_{i \neq j} y_i y_j = -|y|^2$, $|y| = 1$, we have:

$$\text{Var}[\mathbf{e}_x \cdot \mathbf{y}] = \left(\frac{1}{n} + \frac{1}{n^2}\right) |\mathbf{e}_x|^2 \approx \frac{1}{n} |\mathbf{e}_x|^2.$$

Theorem 3 implies that the error vector tends to be uniformly distributed on the $(n-1)$ -sphere. For any unit vector \mathbf{y} on that sphere, the variance of the inner product is the same and converges to 0 as the dimension n increases.

In our case, let Y be a hidden representation of a sample obtained by random linear transformation of the original data, i.e., $Y = AX + \mathbf{b}$. As long as A and \mathbf{b} follow normal distribution (or any distribution that has a zero mean), we have: $\mathbb{E} Y \approx 0$, $|M(Y)|^2 \approx \frac{1}{n} |Y|^2$ and $|E_Y| \approx |Y|$. I.e., the magnitude of Y 's error vector E_Y is significantly larger than Y 's element-wise mean $M(Y)$. Then denoting V as the distance covariance function, it is appropriate to assume:

- $V(X, E) \approx 0$ and $V(M(Y), E) \approx 0$, i.e., the error vector of Y 's permutation is nearly independent with Y 's element-wise mean or X .
- $V(\pi[Y]) = V(M(Y) + E_Y) > V(M(Y))$, i.e., the distance variance of $\pi[Y]$ is smaller than the distance variance of $M(Y)$ due to the magnitude of error vector is large.

Under those assumptions and by the property of distance covariance, we have:

$$\begin{aligned} \mathbb{E}_{\pi} \text{Dcor}(X, \pi[Y]) &= V^2(X, \pi[Y]) / \sqrt{V^2(X)V^2(\pi[Y])} \\ &\lesssim V^2(X, M(Y)) / \sqrt{V^2(X)V^2(M(Y))} \\ &= \text{Dcor}(X, M(Y)). \end{aligned} \quad (7)$$

Since Y is a random projection of X , then we have:

$$\begin{aligned} \mathbb{E}_{\pi, A} \text{Dcor}(X, \pi[AX]) &\lesssim \mathbb{E}_{\pi, A} \text{Dcor}(X, M(AX)) \\ &= \mathbb{E}_{B \in \mathbb{R}^{n \times 1}} \text{Dcor}(X, BX), \end{aligned} \quad (8)$$

where both A and B follow random normal distribution.

By now, we can conclude that in the sense of distance correlation, applying random permutation on hidden representations usually leaks less information than reducing the hidden representation to only one dimension.

5.3.3. Simulated Experiment

In order to verify the above analysis, we conduct simulated experiments on the following four kinds of data distributions whose dimensions are all 100.

- *Normal distribution.* Each data value is drawn from $\mathcal{N}(0, 1)$ independently.
- *Uniform distribution.* Each data value is drawn from $\mathcal{U}(0, 1)$ independently.

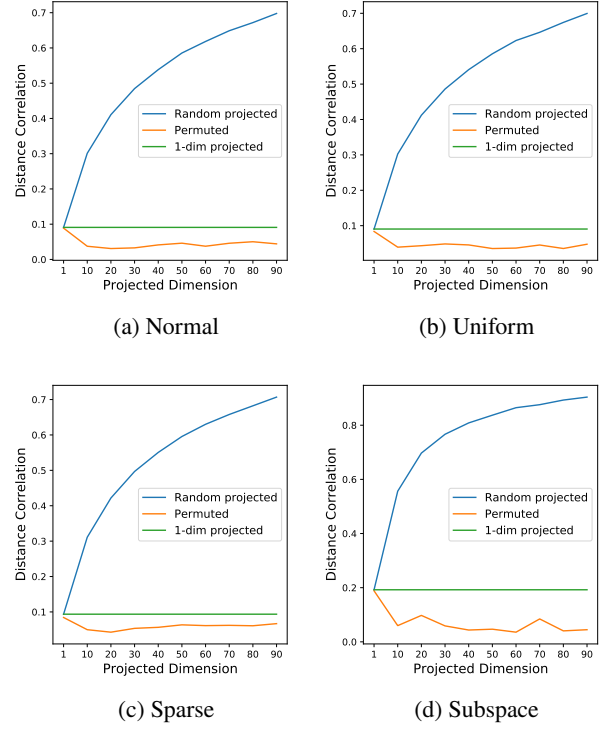


Figure 5: Simulated experiments on different distribution. Blue: Random linear transformation; Green: random linear transformation to 1 dimension; Orange: Random permutation

- *Sparse distribution,* Each data value has a probability of 0.1 to be 1 and otherwise being 0.
- *Subspace distribution,* Each data sample is distributed near to a 20-dimensional subspace and with a error drawn from $\mathcal{N}(0, 1)$. Each data sample can be represented by $X = AH + E$, where $H \in \mathbb{R}^{20}$ and $H_i \sim \mathcal{N}(0, 1)$, $A \in \mathbb{R}^{20 \times 100}$, $A_{i,j} \sim \mathcal{N}(0, \frac{1}{20^2})$, and $E \in \mathbb{R}^{100}$, $E_i \sim \mathcal{N}(0, 0.1)$.

For each distribution, we simulate 10,000 samples. For random linear transformation (labeled as random projected), we use Theorem 2 to accurately calculate the expected distance correlation. And for random permutation, we use Brownian distance covariance [44] to estimate the distance correlation using 10,000 repeated samplings in order to reduce estimation error.

The results in Figure 5 support our analysis. The distance correlation of permuted data is constantly smaller than the distance correlation of 1-dimensional transformed data. The results also show that the distance correlation of linear transformation is strongly affected by the distribution of the original data. In the subspace case, the distance correlation is significantly higher than other distributions. However, after applying random permutations on hidden representations, the distance correlation drops to a level below 0.1. This shows random permutation is more resilient when the original data's distribution is special.

6. Experiments

In this section, we conduct experiments on both simulated data and real-world datasets. We demonstrate the efficiency of our method via benchmarking our method on Logistic Regression (LR) and Deep Neural Network (DNN) models, and compare with the state-of-the-art cryptographic methods. We also demonstrate the security of our method via computing distance correlation and simulating histogram attack on the leaked data.

6.1. Settings

Our implementation is written in Python, and we use NumPy library for both 64-bit integer and float-point computations. We conduct our experiments on a server equipped with a 16-core Intel Xeon CPU and 64Gb RAM. We simulate the WAN setting using Linux’s `tc` command. The bandwidth is set to 80Mbps and the round trip latency is set to 40ms. For all experiments, the data is shared between P_0 and P_1 before testing.

6.2. Benchmarks

We benchmark the running time and network traffic for logistic regression and neural network models using our proposed method, and compare them with ABY3 [33] and SecureNN [48]. We choose the open-source library `rosetta`¹ and `tf-encrypted`² to implement SecureNN and ABY3 respectively. We run all the benchmarks for 10 times and report the average result. To measure the network traffic, we record all the network traffics of our method and use the `tshark` command to monitor the network traffics for ABY3 and SecureNN. We exclude the traffic for TCP packet header via subtracting $64 \cdot N_{packets}$ from the originally recorded bytes. Since we only benchmark the running time and network traffic, we use random data as the input of the models.

Logistic Regression. We benchmark logistic regression model with input dimension in $\{100, 1,000\}$ and batch size in $\{64, 128\}$, for both model training and inference. The benchmark results for logistic regression model are shown in Table 2 and Table 3. Compared with the best results of other methods, our method is about 2~4 times faster for model inference and training. As for network traffic, our method has a reduction of about 35%~55% for model inference and training when the input dimension is 100, and is slightly higher than ABY3 in the case of dimension 1000.

Neural Networks. We also benchmark two fully connected neural networks DNN1 and DNN2 in Table 4 and Table 5. DNN1 is a 3-layer fully connected neural network with an input dimension of 100 and a hidden dimension 50, while DNN2 has an input dimension of 1,000 and a hidden dimension of 500. Compared with logistic regression models, our method has more advantage on neural networks. Compared with the neural networks implemented by SecureNN and ABY3, the speedup of our model against model inference/training is about $1.5 \times \sim 5.5 \times$, and the reduction of network traffic is around 38%~80%.

¹<https://github.com/LatticeX-Foundation/Rosetta>

²<https://github.com/tf-encrypted/tf-encrypted>

Table 2

Running time (s) for LR training/inference.

Dim	batch size		Ours	SecureNN	ABY3
100	64	infer	0.099	0.219	0.5
		train	0.279	0.348	0.534
	128	infer	0.108	0.228	0.5
		train	0.281	0.367	0.539
1000	64	infer	0.132	0.358	0.511
		train	0.294	0.698	0.831
	128	infer	0.114	0.558	0.513
		train	0.334	1.202	0.837

Table 3

Network traffic (Mb) for LR training/inference.

Dim	batch size		Ours	SecureNN	ABY3
100	64	infer	0.103	0.226	0.372
		train	0.209	0.391	0.385
	128	infer	0.202	0.448	0.624
		train	0.413	0.775	0.639
1000	64	infer	0.996	1.072	1.369
		train	1.988	2.581	1.678
	128	infer	1.975	2.134	1.884
		train	3.949	5.121	3.225

Table 4

Running time (s) for DNN inference/training, where DNN1’s architecture is 100-50-relu-1-sigmoid and DNN2’s architecture is 1000-500-relu-1-sigmoid.

	batch size		Ours	SecureNN	ABY3
DNN1	64	infer	0.187	0.682	0.75
		train	0.54	1.292	0.883
	128	infer	0.198	1.097	1.776
		train	0.589	2.083	0.916
DNN2	64	infer	1.047	5.672	1.862
		train	1.864	12.109	3.236
	128	infer	1.262	9.875	3.645
		train	2.577	20.002	5.137

Table 5

Total network traffic (Mb) for DNN inference/training.

	batch size		Ours	SecureNN	ABY3
DNN1	64	infer	0.39	1.984	1.895
		train	0.78	4.05	2.208
	128	infer	0.7	3.891	3.629
		train	1.38	7.902	4.099
DNN2	64	infer	10.69	25.175	17.16
		train	17.97	55.979	35.196
	128	infer	12.54	43.079	36.094
		train	24.84	93.19	47.71

Hidden Layers of Different Size. In order to demonstrate the advantage of our method on non-linear activation functions, we compare our method with ABY3 and SecureNN on fully connected layers of different numbers of hidden units (i.e., output dimension), and report the results in Figure 6, where the input dimension is fixed to 1,000. The result shows that our method tends to have higher speedup and

more communication reductions with the increase of hidden units. The reduction of network traffic increases from $1\times$ to $8\times$ compared to SecureNN and $1.6\times$ to $3.2\times$ compared to ABY3 when the size of layer increases from 1 to 1024. This is because that more units require more non-linear computations. The portion of non-linear computations will be even larger in more complex models like convolutional neural networks. Hence, our method is potentially better on those models.

6.3. Experiments on Real-World Datasets

We also conduct experiments of logistic regression and neural networks on real-world datasets. We train a logistic regression model on the The Gisette dataset³. Gisette dataset contains 50,000 training samples and 5,000 validation samples of dimension 5,000, with labels of -1 or 1.

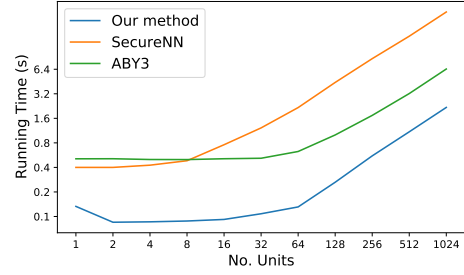
As for neural networks, we train two neural networks on the MNIST [27] dataset. The MNIST dataset contains 50,000 training samples and 5,000 validation samples of dimension 28×28 , with labels of 0 to 9, which we convert into one-hot vectors of dimension 10. We use ReLU for hidden layers and Sigmoid for output layers as activation functions. The first neural network has a hidden layer of size 128, while the second neural network has two hidden layers of size 128 and 32.

Model Performance. We compare our method with the centralized plaintext training and report the accuracy curve of the logistic model in Figure 7 and two neural networks in Figure 8, respectively. The curves of our method and the centralized plaintext training are almost overlapped for all the three models, indicating that our method does not suffer from accuracy loss. This is because the main accuracy loss for our method is the conversion between float-point and fixed-point. However, since we use 64-bit fixed-point integer and precision bits of 23, this loss is very tiny and even negligible for machine learning models.

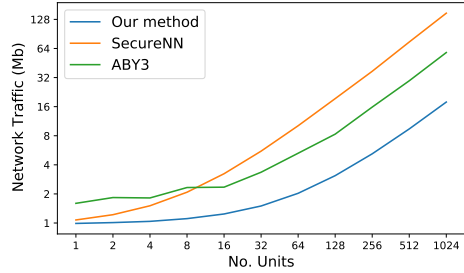
Privacy Leakage. We measure the distance correlation between original training data and the permuted hidden representation (which is obtained by P_2) of the above neural network models, compare it with the no-permutation case (like split learning), and report the result in Figure 9. The result shows that without permutation, the distance correlation is at a high value of about 0.8. After applying permutation, the distance correlation decreases to about 0.03, which indicates that almost no information about original data is leaked.

Simulated Attack. We simulate the histogram attack proposed in Section 5. The setting is that the adversary has 3,000 leaked images with the same distribution as the original MNIST training dataset and also has 3,000 hidden representations with dimension 128. We extract ten hidden representations of digit 1 and find the most similar 10 samples via comparing the histogram distances with the leaked images.

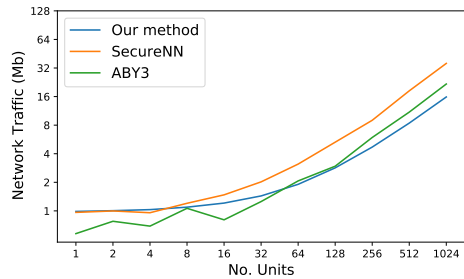
Figure 10 is the result of the histogram attack when the adversary directly gets the hidden representations. The similar images to digit 1 found by the adversary are almost



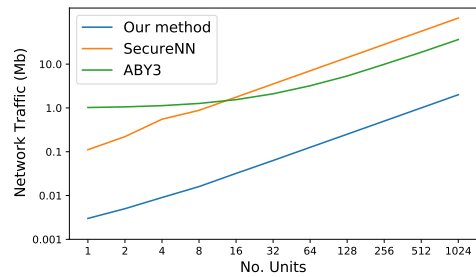
(a) Running time



(b) Total network traffic



(c) Network traffic between P_0 and P_1



(d) Network traffic of P_2

Figure 6: Running time and network communication on fully-connected layers with different number of units. Blue: Our method; Orange: SecureNN; Green: ABY3.

the same as the original image. Moreover, the thickness and the rotation angles of these similar images are close to the original image.

Figure 11 shows the result when permutation is applied in different batch sizes. When batch size is one, it seems that the attack succeeds in the 7-th hidden representation. A possible reason is that the 7-th image is very dark since the white pixels are rare, causes the absolute values of elements

³<https://archive.ics.uci.edu/ml/datasets/Gisette>

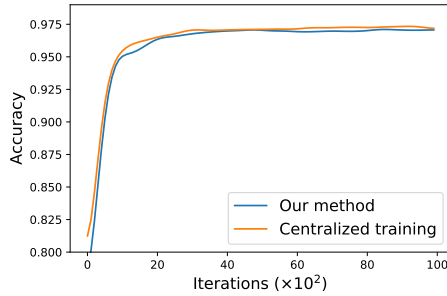


Figure 7: Validation accuracy of logistic regression on Gisette dataset. Orange: Centralized plaintext model; Blue: Our method.

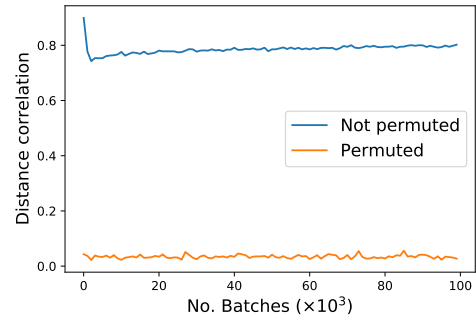


Figure 9: Distance correlation between leaked data and original data. Blue: Not permuted; Orange: Permuted.

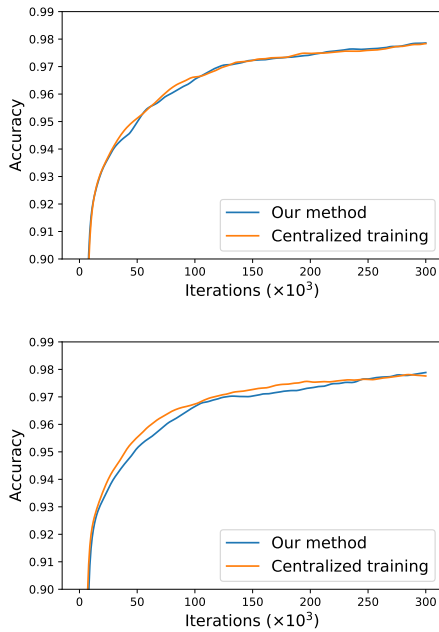


Figure 8: Validation accuracy of neural network 784-128-10 and 784-128-32-10 on MNIST dataset. Orange: Centralized plaintext model; Blue: Our method.

in hidden representations very small. When batch size is 1, the set of elements corresponding to the sample is unchanged after permutation and their absolute values are still very small. Hence, through histogram attack, images with large portion of black pixels are found, and most of them are of digit 1. However, when the batch size is more than 1, multiple samples are shuffled together, the result tends to be completely random and has no relation with the original image.

7. Conclusion and Future Work

In this paper, we propose a privacy-preserving machine learning system via combining arithmetic sharing and random permutation. We exploit the element-wise property of many activation functions, and use random permutation to

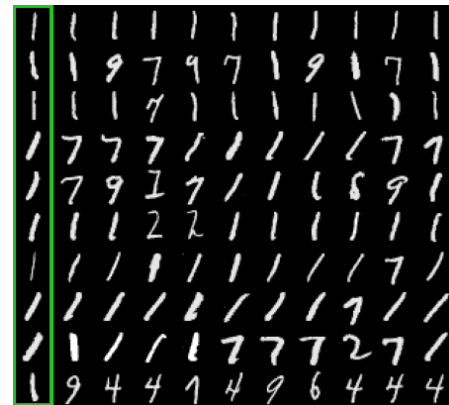


Figure 10: The hidden representations are revealed without permutation. The left column is the original image, and the other 10 columns are the most similar samples find in the leaked data.

let one party do the computation without revealing information about the original data. Through this, our method achieves better efficiency than state-of-the-art cryptographic solutions. We adopt distance correlation to quantify the privacy leakage, illustrating that our method leaks very little information about the original data, while other non-provable secure methods leak information highly correlated to the original data.

In the future, we would like to further apply random permutation to other privacy-preserving machine learning models. We are also interested in developing practical secure methods under other security settings such as the malicious secure setting.

8. Acknowledgement

This work was supported in part by the National Key R&D Program of China (No. 2018YFB1403001) and National Natural Science Foundation of China (No. 62172362, No. 72192823).

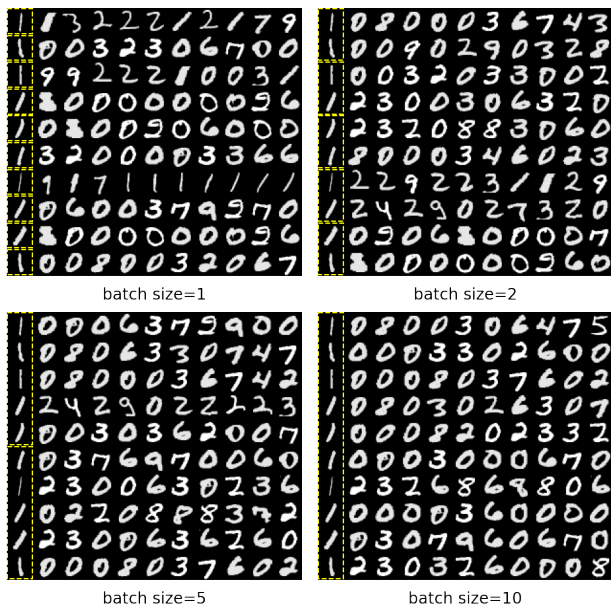


Figure 11: Permutation is performed with batch size in $\{1, 2, 5, 10\}$. Each sample's hidden representation is shuffled within its batch (represented by yellow dashed rectangles).

References

- [1] Abuadba, S., Kim, K., Kim, M., Thapa, C., Çamtepe, S.A., Gao, Y., Kim, H., Nepal, S., 2020. Can we use split learning on 1d CNN models for privacy preserving training?, in: Sun, H., Shieh, S., Gu, G., Ateniese, G. (Eds.), ASIA CCS '20: The 15th ACM Asia Conference on Computer and Communications Security, Taipei, Taiwan, October 5-9, 2020, ACM. pp. 305–318. URL: <https://doi.org/10.1145/3320269.3384740>, doi:10.1145/3320269.3384740.
- [2] Beaver, D., 1991. Efficient multiparty protocols using circuit randomization, in: Feigenbaum, J. (Ed.), Advances in Cryptology - CRYPTO '91, 11th Annual International Cryptology Conference, Santa Barbara, California, USA, August 11-15, 1991, Proceedings, Springer. pp. 420–432. URL: https://doi.org/10.1007/3-540-46766-1_34, doi:10.1007/3-540-46766-1_34.
- [3] Bingham, E., Mannila, H., 2001. Random projection in dimensionality reduction: applications to image and text data, in: Proceedings of the seventh ACM SIGKDD international conference on Knowledge discovery and data mining, pp. 245–250.
- [4] Byali, M., Chaudhari, H., Patra, A., Suresh, A., 2020. FLASH: fast and robust framework for privacy-preserving machine learning. Proc. Priv. Enhancing Technol. 2020, 459–480. URL: <https://doi.org/10.2478/popets-2020-0036>, doi:10.2478/popets-2020-0036.
- [5] Canetti, R., 2001. Universally composable security: A new paradigm for cryptographic protocols, in: 42nd Annual Symposium on Foundations of Computer Science, FOCS 2001, 14-17 October 2001, Las Vegas, Nevada, USA, IEEE Computer Society. pp. 136–145. URL: <https://doi.org/10.1109/SFCS.2001.959888>, doi:10.1109/SFCS.2001.959888.
- [6] Chaudhari, H., Choudhury, A., Patra, A., Suresh, A., 2019. ASTRA: high throughput 3pc over rings with application to secure prediction, in: Sion, R., Papamanthou, C. (Eds.), Proceedings of the 2019 ACM SIGSAC Conference on Cloud Computing Security Workshop, CCSW@CCS 2019, London, UK, November 11, 2019, ACM. pp. 81–92. URL: <https://doi.org/10.1145/3338466.3358922>, doi:10.1145/3338466.3358922.
- [7] Chaudhari, H., Rachuri, R., Suresh, A., 2020. Trident: Efficient 4pc framework for privacy preserving machine learning, in: 27th Annual Network and Distributed System Security Symposium, NDSS 2020, San Diego, California, USA, February 23-26, 2020, The Internet Society. URL: <https://www.ndss-symposium.org/ndss-paper/trident-efficient-4pc-framework-for-privacy-preserving-machine-learning/>.
- [8] Chen, C., Zhou, J., Wang, L., Wu, X., Fang, W., Tan, J., Wang, L., Liu, A.X., Wang, H., Hong, C., 2021. When homomorphic encryption marries secret sharing: Secure large-scale sparse logistic regression and applications in risk control, in: Proceedings of the 27th ACM SIGKDD Conference on Knowledge Discovery & Data Mining, pp. 2652–2662.
- [9] Courbariaux, M., Bengio, Y., David, J.P., 2014. Training deep neural networks with low precision multiplications. arXiv preprint arXiv:1412.7024.
- [10] Demmler, D., Schneider, T., Zohner, M., 2015. ABY - A framework for efficient mixed-protocol secure two-party computation, in: 22nd Annual Network and Distributed System Security Symposium, NDSS 2015, San Diego, California, USA, February 8-11, 2015, The Internet Society. URL: <https://www.ndss-symposium.org/ndss2015/aby---framework-efficient-mixed-protocol-secure-two-party-computation>.
- [11] Dreier, J., Kerschbaum, F., 2011. Practical privacy-preserving multiparty linear programming based on problem transformation, in: PASSAT/SocialCom 2011, Privacy, Security, Risk and Trust (PASSAT), 2011 IEEE Third International Conference on and 2011 IEEE Third International Conference on Social Computing (SocialCom), Boston, MA, USA, 9-11 Oct., 2011, IEEE Computer Society. pp. 916–924. URL: <https://doi.org/10.1109/PASSAT/SocialCom.2011.19>, doi:10.1109/PASSAT/SocialCom.2011.19.
- [12] Du, W., Atallah, M.J., 2001. Privacy-preserving cooperative statistical analysis, in: 17th Annual Computer Security Applications Conference (ACSAC 2001), 11-14 December 2001, New Orleans, Louisiana, USA, IEEE Computer Society. pp. 102–110. URL: <https://doi.org/10.1109/ACSAC.2001.991526>, doi:10.1109/ACSAC.2001.991526.
- [13] Durstenfeld, R., 1964. Algorithm 235: Random permutation. Commun. ACM 7, 420. URL: <https://doi.org/10.1145/364520.364540>, doi:10.1145/364520.364540.
- [14] Dwork, C., Roth, A., 2014. The Algorithmic Foundations of Differential Privacy.
- [15] Evans, D., Kolesnikov, V., Rosulek, M., 2017. A pragmatic introduction to secure multi-party computation. Foundations and Trends® in Privacy and Security 2.
- [16] Fang, W., Zhao, D., Tan, J., Chen, C., Yu, C., Wang, L., Wang, L., Zhou, J., Zhang, B., 2021. Large-scale secure xgb for vertical federated learning, in: Proceedings of the 30th ACM International Conference on Information & Knowledge Management, pp. 443–452.
- [17] Gentry, C., Boneh, D., 2009. A fully homomorphic encryption scheme. volume 20. Stanford university Stanford.
- [18] Gilad-Bachrach, R., Dowlin, N., Laine, K., Lauter, K.E., Naehrig, M., Wernsing, J., 2016. Cryptonets: Applying neural networks to encrypted data with high throughput and accuracy, in: Balcan, M., Weinberger, K.Q. (Eds.), Proceedings of the 33rd International Conference on Machine Learning, ICML 2016, New York City, NY, USA, June 19-24, 2016, JMLR.org. pp. 201–210. URL: <http://proceedings.mlr.press/v48/gilad-bachrach16.html>.
- [19] Gupta, O., Raskar, R., 2018. Distributed learning of deep neural network over multiple agents. J. Netw. Comput. Appl. 116, 1–8. URL: <https://doi.org/10.1016/j.jnca.2018.05.003>, doi:10.1016/j.jnca.2018.05.003.
- [20] He, Q., Yang, W., Chen, B., Geng, Y., Huang, L., 2020. Transnet: Training privacy-preserving neural network over transformed layer. Proc. VLDB Endow. 13, 1849–1862. URL: <http://www.vldb.org/pvldb/vol13/p1849-he.pdf>.
- [21] Hong, C., Huang, Z., Lu, W., Qu, H., Ma, L., Dahl, M., Mancuso, J., 2020. Privacy-preserving collaborative machine learning on genomic data using tensorflow, in: ACM TUR-C'20: ACM Turing Celebration Conference, Hefei, China, May 22-24, 2020, ACM. pp. 39–44. URL: <https://doi.org/10.1145/3393527.3393535>, doi:10.1145/3393527.3393535.
- [22] Johnson, W.B., Lindenstrauss, J., 1984. Extensions of lipschitz mappings into a hilbert space. Contemporary mathematics 26, 1.

- [23] Juvekar, C., Vaikuntanathan, V., Chandrakasan, A., 2018. GAZELLE: A low latency framework for secure neural network inference, in: 27th USENIX Security Symposium (USENIX Security 18), pp. 1651–1669.
- [24] Knott, B., Venkataraman, S., Hannun, A., Sengupta, S., Ibrahim, M., van der Maaten, L., 2020. Crypten: Secure multi-party computation meets machine learning, in: Proceedings of the NeurIPS Workshop on Privacy-Preserving Machine Learning.
- [25] Koti, N., Pancholi, M., Patra, A., Suresh, A., 2020. SWIFT: super-fast and robust privacy-preserving machine learning. CoRR abs/2005.10296. URL: <https://arxiv.org/abs/2005.10296>, arXiv:2005.10296.
- [26] Kumar, N., Rathee, M., Chandran, N., Gupta, D., Rastogi, A., Sharma, R., 2019. Cryptflow: Secure tensorflow inference. CoRR abs/1909.07814. URL: <http://arxiv.org/abs/1909.07814>, arXiv:1909.07814.
- [27] LeCun, Y., Bottou, L., Bengio, Y., Haffner, P., 1998. Gradient-based learning applied to document recognition. Proceedings of the IEEE 86, 2278–2324.
- [28] Liu, J., Juuti, M., Lu, Y., Asokan, N., 2017. Oblivious neural network predictions via minionn transformations, in: Thuraisingham, B.M., Evans, D., Malkin, T., Xu, D. (Eds.), Proceedings of the 2017 ACM SIGSAC Conference on Computer and Communications Security, CCS 2017, Dallas, TX, USA, October 30 - November 03, 2017, ACM. pp. 619–631. URL: <https://doi.org/10.1145/3133956.3134056>, doi:10.1145/3133956.3134056.
- [29] Maekawa, T., Kawamura, A., Kinoshita, Y., Kiya, H., 2018. Privacy-preserving SVM computing in the encrypted domain, in: Asia-Pacific Signal and Information Processing Association Annual Summit and Conference, APSIPA ASC 2018, Honolulu, HI, USA, November 12–15, 2018, IEEE. pp. 897–902. URL: <https://doi.org/10.23919/APSIPA.2018.8659529>, doi:10.23919/APSIPA.2018.8659529.
- [30] Maekawa, T., Kawamura, A., Nakachi, T., Kiya, H., 2019. Privacy-preserving support vector machine computing using random unitary transformation. IEICE Trans. Fundam. Electron. Commun. Comput. Sci. 102-A, 1849–1855. URL: <https://doi.org/10.1587/transfun.E102.A.1849>, doi:10.1587/transfun.E102.A.1849.
- [31] McMahan, B., Moore, E., Ramage, D., Hampson, S., y Arcas, B.A., 2017. Communication-efficient learning of deep networks from decentralized data, in: Singh, A., Zhu, X.J. (Eds.), Proceedings of the 20th International Conference on Artificial Intelligence and Statistics, AISTATS 2017, 20–22 April 2017, Fort Lauderdale, FL, USA, PMLR. pp. 1273–1282. URL: <http://proceedings.mlr.press/v54/mcmahan17a.html>.
- [32] Mishra, P., Lehmkuhl, R., Srinivasan, A., Zheng, W., Popa, R.A., 2020. Delphi: A cryptographic inference service for neural networks, in: Capkun, S., Roesner, F. (Eds.), 29th USENIX Security Symposium, USENIX Security 2020, August 12–14, 2020, USENIX Association. pp. 2505–2522. URL: <https://www.usenix.org/conference/usenixsecurity20/presentation/mishra>.
- [33] Mohassel, P., Rindal, P., 2018. Aby^3 : A mixed protocol framework for machine learning, in: Lie, D., Mannan, M., Backes, M., Wang, X. (Eds.), Proceedings of the 2018 ACM SIGSAC Conference on Computer and Communications Security, CCS 2018, Toronto, ON, Canada, October 15–19, 2018, ACM. pp. 35–52. URL: <https://doi.org/10.1145/3243734.3243760>, doi:10.1145/3243734.3243760.
- [34] Mohassel, P., Zhang, Y., 2017. Secureml: A system for scalable privacy-preserving machine learning, in: 2017 IEEE Symposium on Security and Privacy, SP 2017, San Jose, CA, USA, May 22–26, 2017, IEEE Computer Society. pp. 19–38. URL: <https://doi.org/10.1109/SP.2017.12>, doi:10.1109/SP.2017.12.
- [35] Paillier, P., 1999. Public-key cryptosystems based on composite degree residuosity classes, in: International conference on the theory and applications of cryptographic techniques, Springer. pp. 223–238.
- [36] Patra, A., Suresh, A., 2020. BLAZE: blazing fast privacy-preserving machine learning, in: 27th Annual Network and Distributed System Security Symposium, NDSS 2020, San Diego, California, USA, February 23–26, 2020, The Internet Society. URL: <https://www.ndss-symposium.org/ndss-paper/blaze-blazing-fast-privacy-preserving-machine-learning/>.
- [37] Regev, O., 2009. On lattices, learning with errors, random linear codes, and cryptography. J. ACM 56, 34:1–34:40. URL: <http://doi.acm.org/10.1145/1568318.1568324>, doi:10.1145/1568318.1568324.
- [38] Riazi, M.S., Weinert, C., Tkachenko, O., Songhori, E.M., Schneider, T., Koushanfar, F., 2018. Chameleon: A hybrid secure computation framework for machine learning applications, in: Kim, J., Ahn, G., Kim, S., Kim, Y., López, J., Kim, T. (Eds.), Proceedings of the 2018 on Asia Conference on Computer and Communications Security, AsiaCCS 2018, Incheon, Republic of Korea, June 04–08, 2018, ACM. pp. 707–721. URL: <https://doi.org/10.1145/3196494.3196522>, doi:10.1145/3196494.3196522.
- [39] Rouhani, B.D., Riazi, M.S., Koushanfar, F., 2018. Deepsecure: scalable provably-secure deep learning, in: Proceedings of the 55th Annual Design Automation Conference, DAC 2018, San Francisco, CA, USA, June 24–29, 2018, ACM. pp. 2:1–2:6. URL: <https://doi.org/10.1145/3195970.3196023>, doi:10.1145/3195970.3196023.
- [40] Rubner, Y., Tomasi, C., Guibas, L.J., 2000. The earth mover’s distance as a metric for image retrieval. Int. J. Comput. Vis. 40, 99–121. URL: <https://doi.org/10.1023/A:1026543900054>, doi:10.1023/A:1026543900054.
- [41] Sabt, M., Achemlal, M., Bouabdallah, A., 2015. Trusted execution environment: what it is, and what it is not, in: 2015 IEEE Trustcom/BigDataSE/ISPA, IEEE. pp. 57–64.
- [42] Sang, Y., Shen, H., Tian, H., 2012. Effective reconstruction of data perturbed by random projections. IEEE Trans. Computers 61, 101–117. URL: <https://doi.org/10.1109/TC.2011.83>, doi:10.1109/TC.2011.83.
- [43] Shamir, A., 1979. How to share a secret. Communications of the ACM 22, 612–613.
- [44] Székely, G.J., Rizzo, M.L., 2009. Brownian distance covariance. The annals of applied statistics 3, 1236–1265.
- [45] Székely, G.J., Rizzo, M.L., Bakirov, N.K., et al., 2007. Measuring and testing dependence by correlation of distances. The annals of statistics 35, 2769–2794.
- [46] Vaidya, J., Clifton, C., 2003. Privacy-preserving k -means clustering over vertically partitioned data, in: Getoor, L., Senator, T.E., Domingos, P.M., Faloutsos, C. (Eds.), Proceedings of the Ninth ACM SIGKDD International Conference on Knowledge Discovery and Data Mining, Washington, DC, USA, August 24 - 27, 2003, ACM. pp. 206–215. URL: <https://doi.org/10.1145/956750.956776>, doi:10.1145/956750.956776.
- [47] Vepakomma, P., Gupta, O., Swedish, T., Raskar, R., 2018. Split learning for health: Distributed deep learning without sharing raw patient data. CoRR abs/1812.00564. URL: <http://arxiv.org/abs/1812.00564>, arXiv:1812.00564.
- [48] Wagh, S., Gupta, D., Chandran, N., 2019. Securenn: 3-party secure computation for neural network training. Proc. Priv. Enhancing Technol. 2019, 26–49. URL: <https://doi.org/10.2478/popets-2019-0035>, doi:10.2478/popets-2019-0035.
- [49] Wong, H.W.H., Ma, J.P.K., Wong, D.P.H., Ng, L.K.L., Chow, S.S.M., 2020. Learning model with error - exposing the hidden model of BAYHENN, in: Bessiere, C. (Ed.), Proceedings of the Twenty-Ninth International Joint Conference on Artificial Intelligence, IJCAI 2020, ijcai.org. pp. 3529–3535. URL: <https://doi.org/10.24963/ijcai.2020/488>, doi:10.24963/ijcai.2020/488.
- [50] Xie, P., Wu, B., Sun, G., 2019. BAYHENN: combining bayesian deep learning and homomorphic encryption for secure DNN inference, in: Kraus, S. (Ed.), Proceedings of the Twenty-Eighth International Joint Conference on Artificial Intelligence, IJCAI 2019, Macao, China, August 10–16, 2019, ijcai.org. pp. 4831–4837. URL: <https://doi.org/10.24963/ijcai.2019/671>, doi:10.24963/ijcai.2019/671.
- [51] Yang, Q., Liu, Y., Chen, T., Tong, Y., 2019. Federated machine learning: Concept and applications. ACM Transactions on Intelligent Systems and Technology (TIST) 10, 1–19.
- [52] Yao, A.C., 1986. How to generate and exchange secrets (extended abstract), in: 27th Annual Symposium on Foundations of Computer

- Science, Toronto, Canada, 27-29 October 1986, IEEE Computer Society, pp. 162–167. URL: <https://doi.org/10.1109/SFCS.1986.25>, doi:10.1109/SFCS.1986.25.
- [53] Yin, H., Mallya, A., Vahdat, A., Alvarez, J.M., Kautz, J., Molchanov, P., 2021. See through gradients: Image batch recovery via gradient-inversion. CoRR abs/2104.07586. URL: <https://arxiv.org/abs/2104.07586>, arXiv:2104.07586.
- [54] Zhang, Q., Wang, C., Wu, H., Xin, C., Phuong, T.V., 2018. Gelu-net: A globally encrypted, locally unencrypted deep neural network for privacy-preserved learning, in: Lang, J. (Ed.), Proceedings of the Twenty-Seventh International Joint Conference on Artificial Intelligence, IJCAI 2018, July 13-19, 2018, Stockholm, Sweden, ijcai.org, pp. 3933–3939. URL: <https://doi.org/10.24963/ijcai.2018/547>, doi:10.24963/ijcai.2018/547.
- [55] Zheng, L., Chen, C., Liu, Y., Wu, B., Wu, X., Wang, L., Wang, L., Zhou, J., Yang, S., 2020. Industrial scale privacy preserving deep neural network. arXiv preprint arXiv:2003.05198 .
- [56] Zheng, L., Zhou, J., Chen, C., Wu, B., Wang, L., Zhang, B., 2021. ASFGNN: automated separated-federated graph neural network. Peer Peer Netw. Appl. 14, 1692–1704. URL: <https://doi.org/10.1007/s12083-021-01074-w>, doi:10.1007/s12083-021-01074-w.
- [57] Zhu, L., Liu, Z., Han, S., 2019. Deep leakage from gradients, in: Wallach, H.M., Larochelle, H., Beygelzimer, A., d’Alché-Buc, F., Fox, E.B., Garnett, R. (Eds.), Advances in Neural Information Processing Systems 32: Annual Conference on Neural Information Processing Systems 2019, NeurIPS 2019, 8-14 December 2019, Vancouver, BC, Canada, pp. 14747–14756. URL: <http://papers.nips.cc/paper/9617-deep-leakage-from-gradients>.